THE EFFECT OF PHASE INSTABILITIES ON THE CORRELATION OF NICKEL ION AND NEUTRON IRRADIATION SWELLING IN SOLUTION ANNEALED 316 STAINLESS STEEL*

ROWCLIFFE A. F. - LEE E. H. - SKLAD P. S.

RADIATION EFFECTS AND MICROSTRUCTURAL ANALYSIS GROUP, METALS AND CERAMICS DIVISION, OAK RIDGE NATIONAL LABORATORY, OAK RIDGE, TENNESSEE 37830 UNITED STATES

SUMMARY

Annealed 316 stainless steel specimens were neutron irradiated to establish steady-state microstructures and then subjected to further high temperature irradiations with 4 MeV Ni ions. It is shown that void growth under neutron irradiation is simulated in ion irradiations carried out at ~180°C above reactor temperature. However, the precipitate microstructure developed during neutron irradiation is unstable during subsequent ion irradiation. As a result, the relative swelling rates at various reactor temperatures are not simulated correctly.

1. INTRODUCTION

In recent years, heavy ion irradiation experiments have greatly extended our knowledge of the nature of displacement damage processes, the nucleation and growth of voids and loops, the stability of phases under irradiation, and the behavior of solutes in point defect concentration gradients. In addition, heavy ion irradiations have been utilized in alloy development programs, generally with two main objectives: (1) to compare the swelling behavior of contending alloys and to optimize compositions and (2) to predict the temperature and fluence dependence of swelling in neutron irradiations. The attainment of a successful simulation of in-reactor behavior is complicated by a wide range of factors pertaining to differences in the physical environment in neutron and heavy ion irradiations. These factors were discussed at the Scottsdale Conference [1]. Since then, several of these factors have been examined in greater detail — e.g., the magnitude of the temperature shift of the swelling maximum with dose rate [2,3], the effect of the injected extra interstitials and the effect of the diffusional spreading of point defects on the spatial distribution

RADIATION EFFECTS AND MICROSTRUCTURAL ANALYSIS GROUP, METALS AND CERAMICS DIVISION, OAK RIDGE NATIONAL LABORATORY, OAK RIDGE, TENNESSEE 37830 UNITED STATES

SUMMARY

Annealed 316 stainless steel specimens were neutron irradiated to establish steady-state microstructures and then subjected to further high temperature irradiations with 4 MeV Ni ions. It is shown that void growth under neutron irradiation is simulated in ion irradiations carried out at ∿180°C above reactor temperature. However, the precipitate microstructure developed during neutron irradiation is unstable during subsequent ion irradiation. As a result, the relative swelling rates at various reactor temperatures are not simulated correctly.

1. INTRODUCTION

In recent years, heavy ion irradiation experiments have greatly extended our knowledge of the nature of displacement damage processes, the nucleation and growth of voids and loops, the stability of phases under irradiation, and the behavior of solutes in point defect concentration gradients. In addition, heavy ion irradiations have been utilized in alloy development programs, generally with two main objectives: (1) to compare the swelling behavior of contending alloys and to optimize compositions and (2) to predict the temperature and fluence dependence of swelling in neutron irradiations. The attainment of a successful simulation of in-reactor behavior is complicated by a wide range of factors pertaining to differences in the physical environment in neutron and heavy ion irradiations. These factors were discussed at the Scottsdale Conference [1]. Since then, several of these factors have been examined in greater detail — e.g., the magnitude of the temperature shift of the swelling maximum with dose rate [2,3], the effect of the injected extra interstitials and the effect of the diffusional spreading of point defects on the spatial distribution of swelling [4,5], the effect of the continuous generation of helium during simulation experiments [6]. The effects of mobile helium have been incorporated in rate theory models [7,8], and with the advent of dual beam accelerator systems, it is now possible to investigate the regimes of gas-assisted swelling and gas-driven swelling [9]. There is now a greatly expanded awareness of the physical factors which must be recognized and accounted for in the interpretation of heavy ion irradiation experiments. However, in attempting to simulate the swelling behavior of complex alloys, the effect of damage rate on phase stability also has to be accounted for. In many alloys, the temperature and dose dependence of swelling is closely related to the development of radiation-induced phases or the radiation-enhanced growth of phases. For a successful simulation, this relationship must be preserved at the higher damage rate and higher temperature of the ion irradiation. To investigate this question of phase stability in simulation experiments, a series of ion irradiations have been carried out on annealed 316 stainless steel (SA 316), both with and without injected helium, and also on specimens of the same material which had been previously neutron irradiated to a fluence of $\sim 8 \times 10^{22}$ n·cm^{-2} (>0.1 MeV). The intent of the prior irradiation (preconditioning) was to establish the precipitate structure, matrix chemistry and void and dislocation sink strengths typical of neutron-irradiated material before commencing nickel-ion irradiation.

2. EXPERIMENTAL RESULTS

2.1 Neutron Irradiation of SA 316

Specimens of AISI 316 stainless steel (Heat M 2783, Table 1) in the form of tubes 6.35 mm OD and 0.38 mm wall thickness were annealed at 1090°C and irradiated to fluences of $\sim 8 \times 10^{22}$ and 12×10^{22} n·cm^{-2} (E > 0.1 MeV) at temperatures of 450, 520, 585, and 675°C. This experiment, in the EBR-II subassembly X098, was carried out by workers at G.E., Sunnyvale [11]. Recent calculations by Gabriel et al. [10] indicate that for 316 stainless steel irradiated in Row 2 of EBR-II, a neutron fluence of 10^{22} n·cm^{-2} (E > 0.1 MeV) will produce a damage level of 5.4 dpa. This conversion

of swelling [4,5], the effect of the continuous generation of helium during simulation experiments [6]. The effects of mobile helium have been incorporated in rate theory models [7,8], and with the advent of dual beam accelerator systems, it is now possible to investigate the regimes of gas-assisted swelling and gas-driven swelling [9]. There is now a greatly expanded awareness of the physical factors which must be recognized and accounted for in the interpretation of heavy ion irradiation experiments. However, in attempting to simulate the swelling behavior of complex alloys, the effect of damage rate on phase stability also has to be accounted for. In many alloys, the temperature and dose dependence of swelling is closely related to the development of radiation-induced phases or the radiation-enhanced growth of phases. For a successful simulation, this relationship must be preserved at the higher damage rate and higher temperature of the ion irradiation. To investigate this question of phase stability in simulation experiments, a series of ion irradiations have been carried out on annealed 316 stainless steel (SA 316), both with and without injected helium, and also on specimens of the same material which had been previously neutron irradiated to a fluence of $\sim 8 \times 10^{22}$ n·cm^{-2} (>0.1 MeV). The intent of the prior irradiation (preconditioning) was to establish the precipitate structure, matrix chemistry and void and dislocation sink strengths typical of neutron-irradiated material before commencing nickel-ion irradiation.

2. EXPERIMENTAL RESULTS

2.1 Neutron Irradiation of SA 316

Specimens of AISI 316 stainless steel (Heat M 2783, Table 1) in the form of tubes 6.35 mm OD and 0.38 mm wall thickness were annealed at 1090°C and irradiated to fluences of $\sim 8 \times 10^{22}$ and 12×10^{22} n·cm^{-2} (E > 0.1 MeV) at temperatures of 450, 520, 585, and 675°C. This experiment, in the EBR-II subassembly X098, was carried out by workers at G.E., Sunnyvale [11]. Recent calculations by Gabriel et al. [10] indicate that for 316 stainless steel irradiated in Row 2 of EBR-II, a neutron fluence of 10^{22} n·cm^{-2} (E > 0.1 MeV) will produce a damage level of 5.4 dpa. This conversion factor will be used in making comparisons between neutron irradiation and ion irradiation swelling rates.

Volume swelling is plotted as a function of irradiation temperature in Fig. 1. A major swelling peak occurred at ~585°C with a swelling rate of ~0.56%/dpa, and a second smaller peak developed at ~450°C with a swelling rate of ~0.19%/dpa. These data were presented earlier by Appleby et al. [12]. Typical microstructures after irradiation to 8×10^{22} n·cm^{-2} are presented in Fig. 2 and the microstructural data summarized in Table 2. At 450°C, the void number density was $\sim 8 \times 10^{14}$ cm^{-3} and the dislocation structure consisted of a mixture of unfaulted loops and open network dislocations. Void nucleation was complete at this fluence and during further neutron irradiation to a fluence of $\sim 12 \times 10^{22}$ n·cm^{-2}, swelling occurred by void growth at constant number density. At the lower fluence some small carbide particles developed, but the dominant mode of precipitation consisted of a uniform dispersion of γ' particles ~10 nm diam. The number density was $\sim 10^{15}$ cm^{-3} and the precipitate volume fraction ~0.5%. Based upon the work of Brager and Garner [13] on cold-worked specimens of the same heat, this phase probably has the composition Ni_3Si.

*Research sponsored by the Division of Reactor Research and Technology, U. S. Department of Energy under contract W-7405-eng-26 with the Union Carbide Corporation.

After irradiation at 585°C the microstructure was dominated by voids >100 nm diam associated with plate-shaped precipitates of comparable dimensions. A family of smaller voids not associated with precipitates was also present. At this temperature, the γ' phase could not be detected. During further neutron irradiation to a fluence of $\sim 12 \times 10^{22}$ n·cm^{-2}, swelling occurred through the growth of all size classes, the void number density remaining constant. The plate-shaped phase was found to have an fcc structure with a lattice parameter of ~ 1.1 nm (i.e., it was iso-structural with $M_{23}C_6$). Energy-dispersive x-ray analysis of particles extracted on carbon films showed that the composition of these particles (in weight percent) was 15 Fe—32 Cr—33 Ni—14 Mo—6 Si. (Carbon cannot be determined by this technique and a knowledge of its concentration could change these values slightly.) The majority of the $M_{23}C_6$ particles examined were found to have the standard cube-on-cube orientation relationship with the matrix. Rod-shaped Laves phase particles were also identified.

2.2 Nickel-ion irradiation of SA 316

Archive specimens of the annealed M2783 material were irradiated in the range 500—735°C with 4 MeV Ni^{+2} ions at a peak displacement rate of 4×10^{-3} dpa s^{-1}. Displacements were calculated using the EDEP-1 code and a value of 40 eV for the effective threshold energy. Specimens were irradiated (a) without helium, (b) with 5 at. ppm He uniformly pre-injected at 25°C, and (c) with helium injected simultaneously with the nickel ions at a rate of 0.4 at. ppm/dpa. Transmission electron microscopy (TEM) measurements were carried out at the peak damage depth. The main objective of these experiments was to determine whether or not the continuous generation of helium would produce the phenomenon of precipitate-void association observed in high-temperature neutron irradiations. Specimens were bombarded to a peak dose of 100 dpa; swelling measurements made at peak damage depth are shown in Fig. 3. At 650°C the void number density was $\sim 1.5 \times 10^{14}$ cm^{-3} in both preinjected and simultaneously injected specimens; in the absence of helium the void number density was $\sim 7 \times 10^{13}$ cm^{-3}. In all three cases, precipitation was very limited over the entire temperature range and bore very little resemblance to the structures developed during neutron irradiation. The formation of γ' could not be detected and carbide formation was restricted to isolated particles ~ 20 nm diam.

Disks, 3 mm diam, were spark-cut from tubes which had been neutron irradiated to a fluence of $\sim 8 \times 10^{22}$ n·cm^{-2} at 450 and 585°C. After grinding flat, specimens were prepared for ion irradiation by vibratory polishing on successively finer abrasives and final electropolishing to remove all mechanical damage. Ion irradiations of these preconditioned specimens were carried out over the temperature range 500 to 750°C to peak damage levels of 30 and 60 dpa. The swelling data for specimens preconditioned at 450°C are shown in Table 3 and plotted in Fig. 4. A maximum in swelling rate occurred at 650°C. The void size distribution and dislocation density were determined at each temperature after irradiation to 60 dpa, Fig. 5. During ion irradiation at 735°C, the void number density and the total swelling decreased to below the neutron irradiated value. During ion irradiation at 550°C, additional void nucleation occurred. At intermediate temperatures of 600 and 650°C, the void number density produced during neutron irradiation did not change and growth occurred of all void size classes. The shift in the void size distribution which occurred during ion irradiation to 60 dpa at 600 or 650°C was qualitatively similar to the shift in size distribution which occurred during neutron irradiation at 450°C over the fluence range from 8 to 12×10^{22} n·cm^{-2} (Fig. 6). During ion irradiation at 600 or 650°C, the dislocation structure changed from a predominantly loop character to a more open network and the total dislocation density decreased slightly. Thus, for the void component of the microstructure, ion irradiation at 600—650°C produced a good simulation of the behavior observed during high fluence neutron irradiation at 450°C. However, dark-field TEM examination showed that the γ' particles which had developed during reactor irradiation at 450°C underwent dissolution during the initial 30 dpa ion irradiation at all ion irradiation temperatures. The small

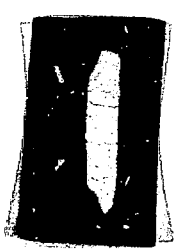

these experiments was to determine whether or not the continuous generation of helium would produce the phenomenon of precipitate-void association observed in high-temperature neutron irradiations. Specimens were bombarded to a peak dose of 100 dpa: swelling measurements made at peak damage depth are shown in Fig. 3. At 650°C the void number density was $\sim 1.5 \times 10^{14}$ cm^{-3} in both preinjected and simultaneously injected specimens; in the absence of helium the void number density was $\sim 7 \times 10^{13}$ cm^{-3}. In all three cases, precipitation was very limited over the entire temperature range and bore very little resemblance to the structures developed during neutron irradiation. The formation of γ' could not be detected and carbide formation was restricted to isolated particles $\sim$20 nm diam.

Disks, 3 mm diam, were spark-cut from tubes which had been neutron irradiated to a fluence of $\sim 8 \times 10^{22}$ n·cm^{-2} at 450 and 585°C. After grinding flat, specimens were prepared for ion irradiation by vibratory polishing on successively finer abrasives and final electropolishing to remove all mechanical damage. Ion irradiations of these preconditioned specimens were carried out over the temperature range 500 to 750°C to peak damage levels of 30 and 60 dpa. The swelling data for specimens preconditioned at 450°C are shown in Table 3 and plotted in Fig. 4. A maximum in swelling rate occurred at 650°C. The void size distribution and dislocation density were determined at each temperature after irradiation to 60 dpa, Fig. 5. During ion irradiation at 735°C, the void number density and the total swelling decreased to below the neutron irradiated value. During ion irradiation at 550°C, additional void nucleation occurred. At intermediate temperatures of 600 and 650°C, the void number density produced during neutron irradiation did not change and growth occurred of all void size classes. The shift in the void size distribution which occurred during ion irradiation to 60 dpa at 600 or 650°C was qualitatively similar to the shift in size distribution which occurred during neutron irradiation at 450°C over the fluence range from 8 to 12 $\times 10^{22}$ n·cm^{-2} (Fig. 6). During ion irradiation at 600 or 650°C, the dislocation structure changed from a predominantly loop character to a more open network and the total dislocation density decreased slightly. Thus, for the void component of the microstructure, ion irradiation at 600–650°C produced a good simulation of the behavior observed during high fluence neutron irradiation at 450°C. However, dark-field TEM examination showed that the γ' particles which had developed during reactor irradiation at 450°C underwent dissolution during the initial 30 dpa ion irradiation at all ion irradiation temperatures. The small carbide particles produced during neutron irradiation appeared to be unaffected by the subsequent ion irradiation.

The additional swelling produced during nickel-ion irradiation of specimens previously neutron irradiated at 585°C is plotted in Fig. 7, and the microstructural data are summarized in Table 3. The behavior was radically different from that observed for the material preconditioned at 450°C. For ion temperatures of 625, 650, and 700°C, the swelling rate, although initially high, eventually decreased with increasing dose. During ion irradiation to 30 dpa further void nucleation occurred and a new population of voids developed with an average size of $\sim$50 nm. During further irradiation to 60 dpa, a reduction in void number density occurred and examination of the void size distribution indicated that although the larger void size classes were growing, shrinkage occurred of voids with diameters below $\sim$30 nm. During these irradiations, the dislocation density was slightly increased (Fig. 8). During nickel-ion irradiation at 750°C, the void number density remained constant and the average void diameter increased. The dislocation density was unchanged, and thus an ion temperature of 750°C appears to be in the correct range to simulate the behavior of the void component of the microstructure during neutron irradiation at 585°C. However, the situation regarding the precipitate microstructure was far less satisfactory. During ion irradiations at temperatures from 600 to 750°C, the large $M_{23}C_6$ particles formed during neutron irradiation, underwent gradual dissolution. Accurate measurements of the dissolution rate were not possible because of the inhomogeneity of the initial precipitate distribution. It was estimated, however, that approximately 75% of the $M_{23}C_6$ phase has dissolved after a dose of 60 dpa at all temperatures (Fig. 9). The temperature dependence of swelling rate for specimens preconditioned at both temperatures is shown in Fig. 10. For the specimens preconditioned at 450°C these rates were obtained by a straight-line extrapolation through the origin of Fig. 4. For specimens preconditioned at 585°C, the swelling rates were calculated from the slope of the line joining the 30 and 60 dpa data points in Fig. 7 and, therefore, represent the swelling rates after appreciable dissolution of the $M_{23}C_6$ had occurred.

3. DISCUSSION

carbide particles produced during neutron irradiation appeared to be unaffected by the subsequent ion irradiation.

The additional swelling produced during nickel-ion irradiation of specimens previously neutron irradiated at 585°C is plotted in Fig. 7, and the microstructural data are summarized in Table 3. The behavior was radically different from that observed for the material preconditioned at 450°C. For ion temperatures of 625, 650, and 700°C, the swelling rate, although initially high, eventually decreased with increasing dose. During ion irradiation to 30 dpa further void nucleation occurred and a new population of voids developed with an average size of ∿50 nm. During further irradiation to 60 dpa, a reduction in void number density occurred and examination of the void size distribution indicated that although the larger void size classes were growing, shrinkage occurred of voids with diameters below ∿30 nm. During these irradiations, the dislocation density was slightly increased (Fig. 8). During nickel-ion irradiation at 750°C, the void number density remained constant and the average void diameter increased. The dislocation density was unchanged, and thus an ion temperature of 750°C appears to be in the correct range to simulate the behavior of the void component of the microstructure during neutron irradiation at 585°C. However, the situation regarding the precipitate microstructure was far less satisfactory. During ion irradiations at temperatures from 600 to 750°C, the large $M_{23}C_6$ particles formed during neutron irradiation, underwent gradual dissolution. Accurate measurements of the dissolution rate were not possible because of the inhomogeneity of the initial precipitate distribution. It was estimated, however, that approximately 75% of the $M_{23}C_6$ phase has dissolved after a dose of 60 dpa at all temperatures (Fig. 9). The temperature dependence of swelling rate for specimens preconditioned at both temperatures is shown in Fig. 10. For the specimens preconditioned at 450°C these rates were obtained by a straight-line extrapolation through the origin of Fig. 4. For specimens preconditioned at 585°C, the swelling rates were calculated from the slope of the line joining the 30 and 60 dpa data points in Fig. 7 and, therefore, represent the swelling rates after appreciable dissolution of the $M_{23}C_6$ had occurred.

3. DISCUSSION

Although swelling in SA 316 occurs readily in both neutron and ion irradiations, the differences in microstructural evolution in the two environments are so great that it is probably meaningless to attempt a correlation between swelling in the two environments in terms of a temperature shift and a dose equivalence factor. Under neutron irradiation the tendency to form a swelling peak at ∿450°C is probably the result of the depletion of nickel and silicon from the matrix to form γ'. The main swelling peak at ∿585°C coincides with the formation of large $M_{23}C_6$ particles enriched in nickel and silicon. The precipitation of this phase has two effects: (1) the matrix becomes depleted in Ni, Si, C, and Mo, and (2) the particle-matrix interface appears to provide a favorable site for the nucleation of gas-stabilized void embryos at high temperature. These precipitation phenomena have not been observed during nickel-ion irradiation of SA 316 either without helium or with preinjected helium. The introduction of helium simultaneously with the nickel ions does not improve the simulation since the precipitation phenomena described above do not occur. The details of the effects of the method of helium injection on the void microstructure and swelling rate cannot be deduced from the single dose experiments carried out here. However, no evidence could be found for double peak swelling behavior in the simultaneous helium injection experiment.

In spite of the failure to reproduce in-reactor precipitation behavior, the results of ion irradiation lead to the correct qualitative prediction that SA 316 will swell fairly rapidly under neutron irradiation. For other alloys,

the effects of precipitation and continuous helium generation may combine in such a way that even such qualitative predictions may be quite misleading. For example, Lee et al. [6] reported that voids could not be detected in a 316 alloy modified with titanium and silicon additions, after preinjection with helium and irradiation with nickel ions to high doses. However, swelling occurred quite readily in the same alloy during low fluence neutron irradiation. The importance of correctly simulating the continuous generation of helium in this alloy was demonstrated by the fact that swelling did occur when ion bombardment was carried out with simultaneous helium injection in a dual ion beam facility.

The technique of preconditioning was adopted with the intention of overcoming these deficiencies by a prior reactor irradiation to establish the appropriate void and dislocation microstructure and to allow a steady-state situation to develop with regard to solute segregation and precipitation. In order to use ion irradiations to successfully simulate the swelling that occurs under neutron irradiation two criteria have to be met. Firstly, there should be an equivalent ion irradiation temperature at which the fluence dependent microstructural changes which occur during neutron irradiation are correctly reproduced. Secondly, the ratio of the swelling rates at any two neutron irradiation temperatures should be reproduced at the two corresponding equivalent ion irradiation temperatures. The results obtained will now be discussed in terms of these criteria.

During neutron irradiation at 450°C, void number density and dislocation density do not change appreciably for fluences between 8 and 12 $\times 10^{22}$ n·cm^{-2} and swelling proceeds by the growth of all void size classes. During nickel-ion irradiation at 600 and 650°C, of specimens previously neutron irradiated at 450°C to $\sim 8 \times 10^{22}$ n·cm^{-2}, the void microstructure evolved in a similar fashion, although some relaxation of the original dislocation structure occurred. Outside this temperature range, constant void number density was not maintained during ion irradiation. Thus the first criterion for a microstructural simulation is fairly well met over the ion irradiation temperature range 600–650°C. During neutron irradiation, the void and dislocation sink strengths combine to produce a swelling peak at 450°C and during subsequent ion irradiation this microstructure develops a maximum swelling rate at 650°C. It seems, therefore, that a good simulation of the swelling behavior under neutron irradiation occurs during ion irradiation at 650°C and that a temperature shift of ~200°C is appropriate for a damage rate change of a factor of $\sim 10^3$. At these equivalent temperatures, equal increments of swelling are produced by a neutron irradiation of 10^{22} n·cm^{-2} (E > 0.1 MeV), i.e., 5.4 dpa, and by an ion irradiation of ~10 dpa. The simulation is deficient in one important microstructural aspect, and that is that the neutron irradiation induced γ' phase undergoes dissolution at all ion irradiation temperatures. Thus, the matrix chemistry established during the neutron irradiation is not maintained during the subsequent ion irradiation and the observed swelling rate is probably lower than it would have been if the γ' precipitates had not dissolved.

During continued neutron irradiation at 585°C from 8 to 12 $\times 10^{22}$ n·cm^{-2}, swelling proceeds at constant void number density. For specimens previously neutron irradiated to 8 $\times 10^{22}$ n·cm^{-2} at 585°C, additional void nucleation occurred during subsequent nickel-ion irradiations at 625, 650, and 700°C, and the dislocation density was slightly increased. At 750°C there was no further nucleation of voids and no detectable increase in dislocation density, and at this ion irradiation temperature the void and dislocation components of the microstructure were similar to those maintained during neutron irradiation at 585°C. However, the precipitate structure developed during neutron irradiation was not maintained during ion irradiation. The dissolution of the $M_{23}C_6$ particles is a complex phenomenon, and the controlling factors are not yet understood. Some possible factors involved are (a) the increased rate of recoil dissolution by [illegible] (b) the temperature shift in solute segregation rate, (c) an increase in solute solubility with

During neutron irradiation at 450°C, void number density and dislocation density do not change appreciably between 8 and 12 × 10^{22} n•cm^{-2} and swelling proceeds by the growth of all void size classes. During nickel-ion irradiation at 600 and 650°C, of specimens previously neutron irradiated at 450°C to ∿8 × 10^{22} n•cm^{-2}, the void microstructure evolved in a similar fashion, although some relaxation of the original dislocation structure occurred. Outside this temperature range, constant void number density was not maintained during ion irradiation. Thus the first criterion for a microstructural simulation is fairly well met over the ion irradiation temperature range 600–650°C. During neutron irradiation, the void and dislocation sink strengths combine to produce a swelling peak at 450°C and during subsequent ion irradiation this microstructure develops a maximum swelling rate at 650°C. It seems, therefore, that a good simulation of the swelling behavior under neutron irradiation occurs during ion irradiation at 650°C and that a temperature shift of ∿200°C is appropriate for a damage rate change of a factor of ∿10^3. At these equivalent temperatures, equal increments of swelling are produced by a neutron irradiation of 10^{22} n•cm^{-2} ($E > 0.1$ MeV), i.e., 5.4 dpa, and by an ion irradiation of ∿10 dpa. The simulation is deficient in one important microstructural aspect, and that is that the neutron irradiation induced γ' phase undergoes dissolution at all ion irradiation temperatures. Thus, the matrix chemistry established during the neutron irradiation is not maintained during the subsequent ion irradiation and the observed swelling rate is probably lower than it would have been if the γ' precipitates had not dissolved.

During continued neutron irradiation at 585°C from 8 to 12 × 10^{22} n•cm^{-2}, swelling proceeds at constant void number density. For specimens previously neutron irradiated to 8 × 10^{22} n•cm^{-2} at 585°C, additional void nucleation occurred during subsequent nickel-ion irradiations at 625, 650, and 700°C, and the dislocation density was slightly increased. At 750°C there was no further nucleation of voids and no detectable increase in dislocation density, and at this ion irradiation temperature the void and dislocation components of the microstructure were similar to those maintained during neutron irradiation at 585°C. However, the precipitate structure developed during neutron irradiation was not maintained during ion irradiation. The dissolution of the $M_{23}C_6$ particles is a complex phenomenon, and the controlling factors are not yet understood. Some possible factors involved are (a) the increased rate of recoil dissolution by displacement cascades, (b) the temperature shift in solute segregation rate, (c) an increase in solute solubility with increasing damage rate, and (c) changes in matrix chemistry due to the point defect coupled flow of solutes out of the peak damage region.

Normally, void swelling develops slowly during an incubation period which is then followed by a higher swelling rate regime. The reverse behavior occurs in the irradiations at 625, 650, and 700°C. Swelling is initially rapid and during the early part of the irradiation additional voids are nucleated. At 650 and 700°C the additional swelling produced during the first 30 dpa ion irradiation is ∿4%. With increasing dose, however, very little additional swelling occurs and there is some reduction in void number density due to the evaporation of small voids. This reduction in swelling rate is thought to be a consequence of the steadily rising concentration of Ni, Si, Mo, and C in the matrix as the $M_{23}C_6$ particles dissolve. The increase in concentration of these elements increases the rate of point defect trapping, thus enhancing recombination, and also modifies the diffusional properties of the matrix. During ion irradiation at 750°C, the vacancy supersaturation is not high enough for additional void nucleation to occur and the swelling versus dose curve extrapolates approximately through the origin. Although the swelling increase during the initial 30 dpa was only just detectable, the actual swelling rate over the range 30 to 60 dpa was higher than at the other ion irradiation temperatures.

Thus in these experiments the microstructural criterion for simulation is fairly well satisfied in terms of the void and dislocation structures. For both neutron irradiation temperatures, there is an equivalent ion temperature at which the void number density is maintained at the steady-state value achieved during the prior neutron irradiation. Some changes occur in the dislocation structure but the relative void and dislocation sink strengths are fairly well maintained at the equivalent temperatures. However, the changes which occur in the precipitate component of the microstructure have a major impact on the second simulation criterion (i.e., the maintenance of the ratio of swelling rates observed at different neutron irradiation temperatures).

The swelling rates at the neutron irradiation temperatures of 585 and 450°C were 0.56%/dpa and 0.19%/dpa, respectively

displacement cascades, (b) the temperature shift in solute segregation [illegible], (c) [illegible] increasing damage rate, and (c) changes in matrix chemistry due to the point defect coupled flow of solutes out of the peak damage region.

Normally, void swelling develops slowly during an incubation period which is then followed by a higher swelling rate regime. The reverse behavior occurs in the irradiations at 625, 650, and 700°C. Swelling is initially rapid and during the early part of the irradiation additional voids are nucleated. At 650 and 700°C the additional swelling produced during the first 30 dpa ion irradiation is ~4%. With increasing dose, however, very little additional swelling occurs and there is some reduction in void number density due to the evaporation of small voids. This reduction in swelling rate is thought to be a consequence of the steadily rising concentration of Ni, Si, Mo, and C in the matrix as the $M_{23}C_6$ particles dissolve. The increase in concentration of these elements increases the rate of point defect trapping, thus enhancing recombination, and also modifies the diffusional properties of the matrix. During ion irradiation at 750°C, the vacancy supersaturation is not high enough for additional void nucleation to occur and the swelling versus dose curve extrapolates approximately through the origin. Although the swelling increase during the initial 30 dpa was only just detectable, the actual swelling rate over the range 30 to 60 dpa was higher than at the other ion irradiation temperatures.

Thus in these experiments the microstructural criterion for simulation is fairly well satisfied in terms of the void and dislocation structures. For both neutron irradiation temperatures, there is an equivalent ion temperature at which the void number density is maintained at the steady-state value achieved during the prior neutron irradiation. Some changes occur in the dislocation structure but the relative void and dislocation sink strengths are fairly well maintained at the equivalent temperatures. However, the changes which occur in the precipitate component of the microstructure have a major impact on the second simulation criterion (i.e., the maintenance of the ratio of swelling rates observed at different neutron irradiation temperatures).

The swelling rates at the neutron irradiation temperatures of 585 and 450°C were 0.56%/dpa and 0.19%/dpa, respectively (i.e., the ratio of peak swelling rates was 3:1). During ion irradiation at the equivalent ion temperatures of 750 and 650°C, the swelling rates were 0.03%/dpa and 0.09%/dpa, respectively (i.e., the ratio of swelling rates was only 1:3). Thus, although a reasonably successful matching of the void microstructure was achieved, the simulation experiments failed, by a factor of 10, to correctly reproduce the relative swelling rates at two neutron irradiation temperatures. These simulation experiments would predict that swelling, in-reactor at 450°C would proceed at three times the rate at 585°C, whereas the reverse is observed. This failure to correctly predict relative swelling rates is directly related to the fact that the precipitate structure developed during neutron irradiation is unstable in the high damage rate ion irradiation environment.

In conclusion, it is now apparent that the precipitation sequences which occur during neutron irradiation of SA 316 are not reproduced during Ni ion irradiation at a damage rate of $\sim 10^{-3}$ dpa s^{-1}. Radiation induced segregation of various solutes occurs during ion irradiation, but the phases which occur in-reactor are not stable. As a result, the role of large precipitates in promoting high temperature void nucleation is not reproduced. In addition, the variations in matrix chemistry over the temperature range of swelling are not the same in the two environments. In SA 316, the presence of helium is not a necessary condition for swelling to occur and the injection of helium simultaneously with the Ni ions does not improve the simulation of in-reactor behavior. (In other related alloys, however, the continuous generation of helium is a necessary condition for void swelling during Ni ion irradiation.)

In terms of the void and dislocation structure, a reasonably good simulation of the changes which occur during high fluence neutron irradiation has been demonstrated through the use of the preconditioning technique. The temperature shift for a damage rate change by a factor of $\sim 10^3$ is in the range 160–200°C. However, even though the void and dislocation components of the microstructure are maintained correctly, the temperature dependence of swelling rate under neutron irradiation is not reproduced under ion irradiation. The phases produced in-reactor are not stable and as dissolution proceeds, the solute concentrations in the matrix are raised. The dissolution of the Ni and Si rich $M_{23}C_6$ phase results in a particularly strong depression of the swelling rate, and the relative swelling rates during neutron irradiation at 585 and 450°C are reversed during subsequent ion irradiations at the equivalent temperatures appropriate for microstructural simulation.

The dependence of phase stability upon damage rate, which precludes the successful simulation of in-reactor swelling for SA 316, will also affect simulation experiments on other alloys which undergo phase transformations during high temperature irradiation. The achievement of quantitative simulation measurements is probably an unrealistic goal, and in some alloys, ion irradiations will undoubtedly give completely misleading indications regarding swelling resistance under neutron irradiation. On the other hand it is possible that in other alloys, phase relationships are maintained over a range of damage rates and temperatures that is sufficient to encompass both neutron and ion irradiation environments. In such cases, swelling behavior may be reasonably well simulated provided that helium is generated continuously at the correct rate.

ACKNOWLEDGMENTS

The work described here formed part of an inter-laboratory correlation program performed within the National Alloy Development Program sponsored by the Division of Reactor Research and Technology, U. S. Department of Energy. The authors wish to acknowledge the contributions made in terms of planning and discussions by F. A. Garner and R. Powell at Hanford Engineering Development Laboratory, T. Lauritzen at General Electric Company, Sunnyvale, and S. Diamond at Westinghouse Advanced Reactors Division. The Ni ion irradiations were carried out by M. B. Lewis at the ORNL 5 MV Van de Graaff facility and the techniques for preparing irradiated specimens for ion irradiation were developed by L. J. Turner and L. T. Gibson at ORNL.

7. REFERENCES

[1] GARNER F. A. - POWELL R. W. - DIAMOND S. - LAURITZEN T. - ROWCLIFFE A. F. - SPRAGUE J. A. - KEEFER D. - Simulation of high fluence swelling behavior in technological materials. Proc. Int. Conf. on Radiation Effects in Breeder Reactor Structural Materials, AIME, Scottsdale, Arizona, USA (1977) 543–569.

[2] PACKAN N. H. - FARRELL K. - STIEGLER J. O. - Correlation of neutron and heavy ion damage, part I. J. Nucl. Mater. 78 (1978) 143–155.

[3] MANSUR L. K. - Correlation of neutron and heavy ion damage, part II. J. Nucl. Mater. 78 (1978) 156–160.

[4] LEE E. H. - MANSUR L. K. - YOO M. H. - Spatial variation in void volume during charged particle bombardment – the effects of injected interstitials. Proc. First Topical Meeting on Fusion Reactor Materials, Miami Beach, Florida (1979). To be published in Journal of Nuclear Materials.

generated continuously at the correct rate.

ACKNOWLEDGMENTS

The work described here formed part of an inter-laboratory correlation program performed within the National Alloy Development Program sponsored by the Division of Reactor Research and Technology, U. S. Department of Energy. The authors wish to acknowledge the contributions made in terms of planning and discussions by F. A. Garner and R. Powell at Hanford Engineering Development Laboratory, T. Lauritzen at General Electric Company, Sunnyvale, and S. Diamond at Westinghouse Advanced Reactors Division. The Ni ion irradiations were carried out by M. B. Lewis at the ORNL 5 MV Van de Graaff facility and the techniques for preparing irradiated specimens for ion irradiation were developed by L. J. Turner and L. T. Gibson at ORNL.

7. REFERENCES

[1] GARNER F. A. - POWELL R. W. - DIAMOND S. - LAURITZEN T. - ROWCLIFFE A. F. - SPRAGUE J. A. - KEEFER D. - Simulation of high fluence swelling behavior in technological materials. Proc. Int. Conf. on Radiation Effects in Breeder Reactor Structural Materials, AIME, Scottsdale, Arizona, USA (1977) 543–569.

[2] PACKAN N. H. - FARRELL K. - STIEGLER J. O. - Correlation of neutron and heavy ion damage, part I. J. Nucl. Mater. 78 (1978) 143–155.

[3] MANSUR L. K. - Correlation of neutron and heavy ion damage, part II. J. Nucl. Mater. 78 (1978) 156–160.

[4] LEE E. H. - MANSUR L. K. - YOO M. H. - Spatial variation in void volume during charged particle bombardment – the effects of injected interstitials. Proc. First Topical Meeting on Fusion Reactor Materials, Miami Beach, Florida (1979). To be published in Journal of Nuclear Materials.

[5] MANSUR L. K. - YOO M. H. - Advances in the theory of radiation effects in metals and alloys. Proc. First Topical Meeting on Fusion Reactor Materials, Miami Beach, Florida (1979). To be published in Journal of Nuclear Materials.

[6] LEE E. H. - ROWCLIFFE A. F. - KENIK E. A. - Effects of Si and Ti on the phase stability and swelling behavior of AISI 316 stainless steel. Proc. of Workshop on Solute Segregation and Phase Stability during Irradiation, Gatlinburg, TN (1978). To be published in Journal of Nuclear Materials.

[7] YOO M. H. - MANSUR L. K. - The inclusion of mobile helium in a rate theory model of void swelling. Proc. First Topical Meeting on Fusion Reactor Materials, Miami Beach, Florida (1979). To be published in Journal of Nuclear Materials.

[8] HALL B. O. - Effect of simultaneous helium injection on nucleation in irradiated metals. Proc. First Topical Meeting on Fusion Reactor Materials, Miami Beach, Florida (1979). To be published in Journal of Nuclear Materials.

[9] HAYNS M. R. - WOOD M. H. - BULLOUGH R. - A theoretical evaluation of dual-beam irradiation experiments. J. Nucl. Mater. 75 (1978) 241.

[10] GABRIEL T. A. - BISHOP B. L. - WIFFEN F. W. - Calculated irradiation response of materials using fission reactor (HFIR, ORR, EBR-II) neutron spectra. ORNL/TM-6361 (1979).

[11] KENFIELD T. A. - APPLEBY W. K. - BELL W. L. - BUSBOOM H. J. - McCLELLAN G. C. - Swelling of types 304, 316, and 321 stainless steels at high fluences in EBR-II. GEFR-00062, General Electric Company (March 1977).

[12] APPLEBY W. K. - BLOOM E. E. - FLINN J. E. - GARNER F. A. - Swelling in neutron-irradiation 300-series stainless

(1979). To be published in Journal of Nuclear Materials.

[5] MANSUR L. K. - YOO M. H. - Advances in the theory of radiation effects in metals and alloys. Proc. First Topical Meeting on Fusion Reactor Materials, Miami Beach, Florida (1979). To be published in Journal of Nuclear Materials.

[6] LEE E. H. - ROWCLIFFE A. F. - KENIK E. A. - Effects of Si and Ti on the phase stability and swelling behavior of AISI 316 stainless steel. Proc. of Workshop on Solute Segregation and Phase Stability during Irradiation, Gatlinburg, TN (1978). To be published in Journal of Nuclear Materials.

[7] YOO M. H. - MANSUR L. K. - The inclusion of mobile helium in a rate theory model of void swelling. Proc. First Topical Meeting on Fusion Reactor Materials, Miami Beach, Florida (1979). To be published in Journal of Nuclear Materials.

[8] HALL B. O. - Effect of simultaneous helium injection on nucleation in irradiated metals. Proc. First Topical Meeting on Fusion Reactor Materials, Miami Beach, Florida (1979). To be published in Journal of Nuclear Materials.

[9] HAYNS M. R. - WOOD M. H. - BULLOUGH R. - A theoretical evaluation of dual-beam irradiation experiments. J. Nucl. Mater. 75 (1978) 241.

[10] GABRIEL T. A. - BISHOP B. L. - WIFFEN F. W. - Calculated irradiation response of materials using fission reactor (HFIR, ORR, EBR-II) neutron spectra. ORNL/TM-6361 (1979).

[11] KENFIELD T. A. - APPLEBY W. K. - BELL W. L. - BUSBOOM H. J. - McCLELLAN G. C. - Swelling of types 304, 316, and 321 stainless steels at high fluences in EBR-II. GEFR-00062, General Electric Company (March 1977).

[12] APPLEBY W. K. - BLOOM E. E. - FLINN J. E. - GARNER F. A. - Swelling in neutron-irradiation 300-series stainless steel. Int. Conf. Radiation Effects in Breeder Reactor Structural Materials, AIME, Scottsdale, Arizona (June 19–23, 1977) 509–527.

[13] BRAGER H. R. - GARNER F. A. - Swelling as a consequence of gamma prime (γ') and $M_{23}(C,Si)_6$ formation in neutron irradiated 316 stainless steel. J. Nucl. Mater. 73 (1978) 9–19.

Table 1

Composition of 316 stainless steel heat M2783 (wt %)

Fe	Cr	Ni	Mo	Si	Ti	Mn	C	N	S	P
Bal	16.8	13.0	2.5	0.47	<0.02	1.8	0.06	0.03	0.02	0.03

3

Table 2

Microstructural data for neutron irradiated SA 316

Neutron Irradiation Temperature °C	Neutron Fluence $n \cdot cm^{-2}$	Average Void Diameter nm	Void Number Density cm^{-3}	Swelling from Profilometry %	Swelling from TEM %	Dislocation Density cm^{-2}
450	7.6×10^{22}	30.8	8.2×10^{14}	2.0	1.6	6×10^{10}
445*	12.5×10^{22}	47.4	7.9×10^{14}	6.5	6.0	—
520	7.6×10^{22}	50.6	1.1×10^{14}	1.2	1.0	3.7×10^{10}
520*	12.5×10^{22}	62.5	4.6×10^{14}	5.7	5.9	—
585	8.1×10^{22}	109.0	3.2×10^{13}	5.2	3.0	5.0×10^{9}
560*	12.5×10^{22}	176.0	3.1×10^{13}	18.4	13.5	—

*Micrographs supplied courtesy of T. Lauritzen, G. E., Sunnyvale.

Table 3

Microstructural data for neutron irradiated and ion irradiated SA 316

Neutron Irradiation Temperature °C	Neutron Fluence $n \cdot cm^{-2}$ ($E > 0.1$ MeV)	Ion Irradiation Temperature °C	Ion Dose dpa	Average Void Diameter nm	Void Number Density cm^{-3}	TEM* $\Delta V/V$ %	Dislocation Density cm^{-2}
450	7.6×10^{22}			30.8	8.2×10^{14}	1.6	6.0×10^{10}
520	7.6×10^{22}			50.6	1.1×10^{14}	1.0	3.7×10^{10}
585	8.1×10^{22}			109.0	3.2×10^{13}	3.0	5.0×10^{9}
450	7.6×10^{22}	600	30	40.6	9.1×10^{14}	2.1	2.4×10^{10}
450	7.6×10^{22}	650	30	46.0	6.6×10^{14}	2 4	1.7×10^{10}
450	7.6×10^{22}	550	60	27.9	1.9×10^{15}	1.0	2.5×10^{10}
450	7.6×10^{22}	600	60	50.3	7.7×10^{14}	3.6	3.5×10^{10}
450	7.6×10^{22}	650	60	53.4	7.5×10^{14}	5.2	1.4×10^{10}
450	7.6×10^{22}	735	60	36.4	2.4×10^{14}	−0.8	5.4×10^{9}
585	8.1×10^{22}	640	30	89.9	5.8×10^{13}	1.7	2.7×10^{10}
585	8.1×10^{22}	657	30	89.6	1.01×10^{14}	4.0	2.9×10^{10}
585	8.1×10^{22}	700	30	100.0	7.0×10^{13}	4.2	2.1×10^{10}

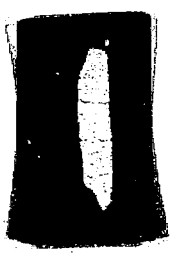

*Micrographs supplied courtesy of T. Lauritzen, G. E., Sunnyvale.

Table 3

Microstructural data for neutron irradiated and ion irradiated SA 316

Neutron Irradiation Temperature °C	Neutron Fluence $n \cdot cm^{-2}$ (E > 0.1 MeV)	Ion Irradiation Temperature °C	Ion Dose dpa	Average Void Diameter nm	Void Number Density cm^{-3}	TEM* ΔV/V %	Dislocation Density cm^{-2}
450	7.6×10^{22}			30.8	8.2×10^{14}	1.6	6.0×10^{10}
520	7.6×10^{22}			50.6	1.1×10^{14}	1.0	3.7×10^{10}
585	8.1×10^{22}			109.0	3.2×10^{13}	3.0	5.0×10^{9}
450	7.6×10^{22}	600	30	40.6	9.1×10^{14}	2.1	2.4×10^{10}
450	7.6×10^{22}	650	30	46.0	6.6×10^{14}	2.4	1.7×10^{10}
450	7.6×10^{22}	550	60	27.9	1.9×10^{15}	1.0	2.5×10^{10}
450	7.6×10^{22}	600	60	50.3	7.7×10^{14}	3.6	3.5×10^{10}
450	7.6×10^{22}	650	60	53.4	7.5×10^{14}	5.2	1.4×10^{10}
450	7.6×10^{22}	735	60	36.4	2.4×10^{14}	−0.8	5.4×10^{9}
585	8.1×10^{22}	640	30	89.9	5.8×10^{13}	1.7	2.7×10^{10}
585	8.1×10^{22}	657	30	89.6	1.01×10^{14}	4.0	2.9×10^{10}
585	8.1×10^{22}	700	30	100.0	7.0×10^{13}	4.2	2.1×10^{10}
585	8.1×10^{22}	750	30	111.0	4.0×10^{13}	0.29	7.3×10^{9}
585	8.1×10^{22}	625	60	104.0	4.8×10^{13}	2.1	1.5×10^{10}
585	8.1×10^{22}	657	60	114.0	6.5×10^{13}	4.8	—
585	8.1×10^{22}	700	60	150.0	4.5×10^{13}	4.9	1.4×10^{10}
585	8.1×10^{22}	750	60	138.0	2.7×10^{13}	1.7	4.9×10^{9}

*Ion irradiation data refers to additional swelling.

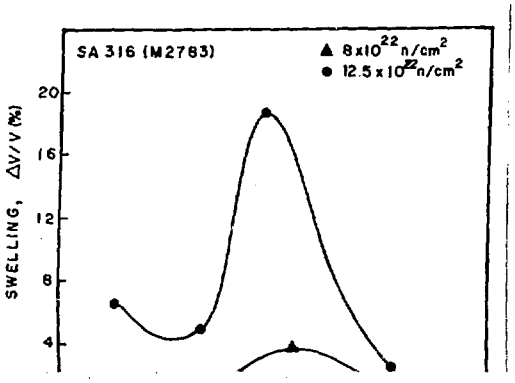

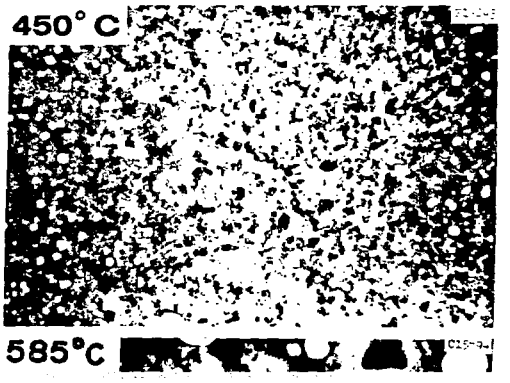

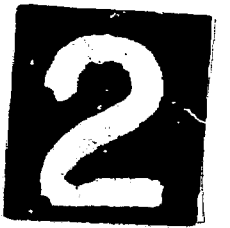

585	8.1 × 10^{22}	625	60	104.0	4.8 × 10^{13}	2.1	1.5 × 10^{10}
585	8.1 × 10^{22}	657	60	114.0	6.5 × 10^{13}	4.8	—
585	8.1 × 10^{22}	700	60	150.0	4.5 × 10^{13}	4.9	1.4 × 10^{10}
585	8.1 × 10^{22}	750	60	138.0	2.7 × 10^{13}	1.7	4.9 × 10^{9}

*Ion irradiation data refers to additional swelling.

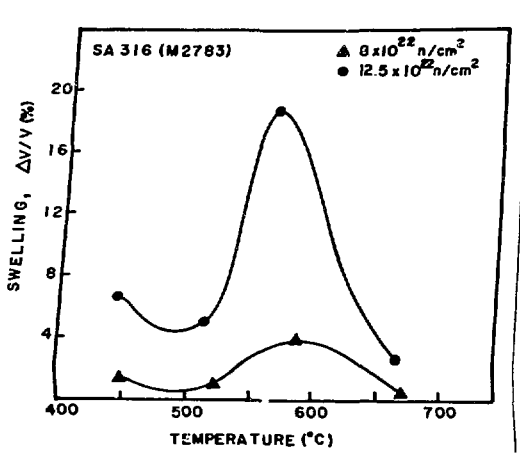

Fig. 1. Swelling calculated from profilometry data for SA 316 stainless steel. From reference [12].

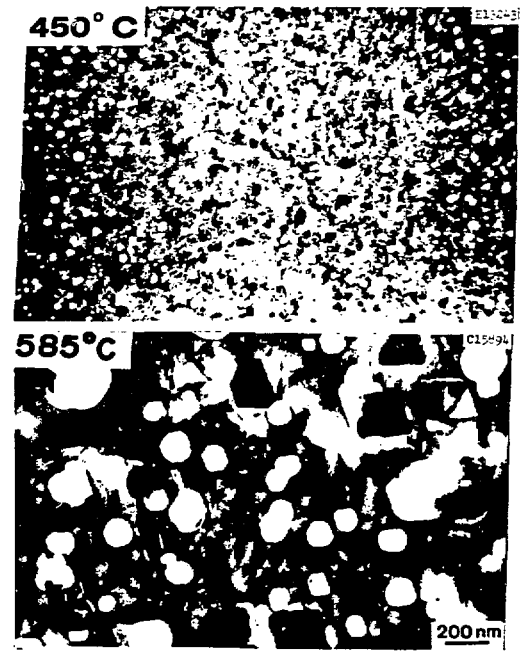

Fig. 2. Transmission electron micrographs of SA 316 neutron irradiated to ~8 × 10^{22} n·cm^{-2} at two temperatures.

3

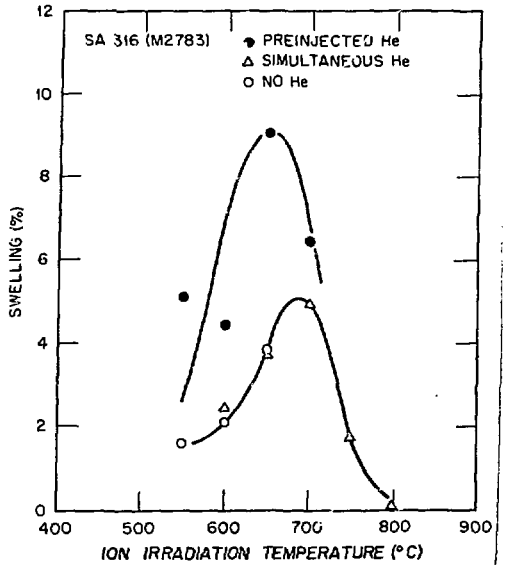

Fig. 3. TEM swelling data for SA 316 irradiated with 4 MeV Ni ions to 100 dpa (a) without helium, (b) with 5 at. ppm preinjected helium, and (c) with helium simultaneously implanted at 0.4 ppm/dpa.

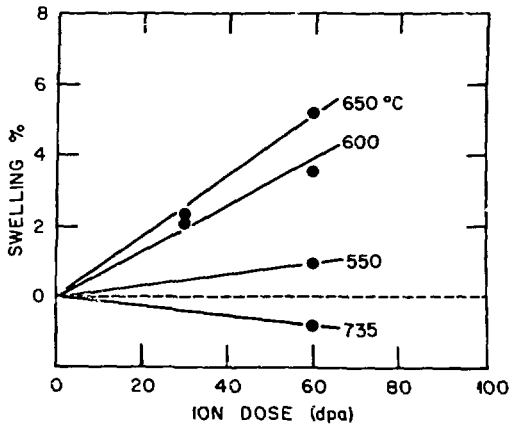

Fig. 4. Additional swelling produced during 4 MeV Ni ion irradiation of SA 316 after prior neutron irradiation at 450°C.

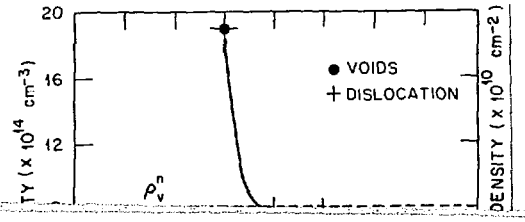

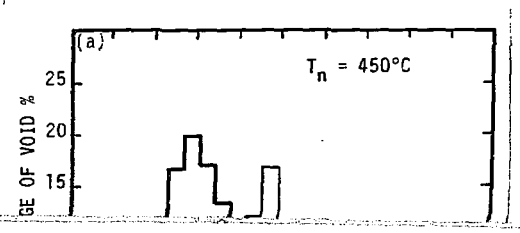

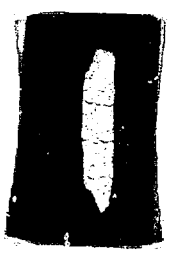

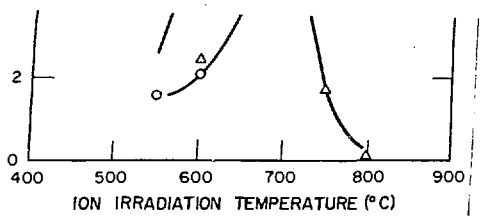

Fig. 3. TEM swelling data for SA 316 irradiated with 4 MeV Ni ions to 100 dpa (a) without helium, (b) with 5 at. ppm preinjected helium, and (c) with helium simultaneously implanted at 0.4 ppm/dpa.

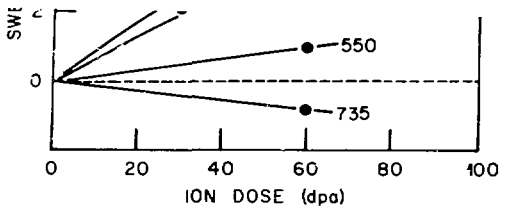

Fig. 4. Additional swelling produced during 4 MeV Ni ion irradiation of SA 316 after prior neutron irradiation at 450°C.

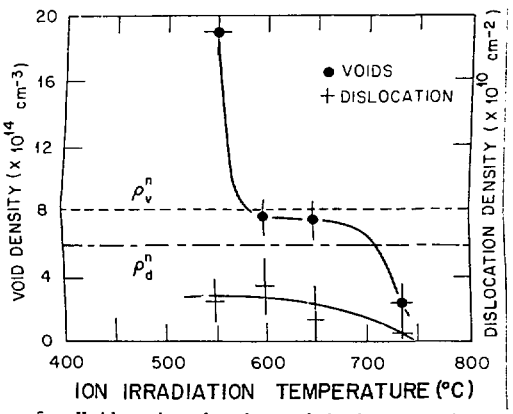

Fig. 5. Void number density and dislocation density for specimens preconditioned at 450°C and Ni ion irradiated to 60 dpa. Broken lines indicate the levels attained during neutron irradiation.

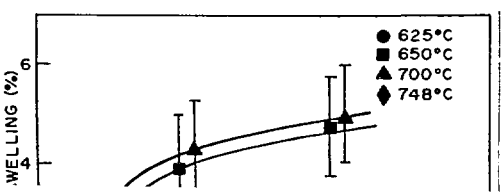

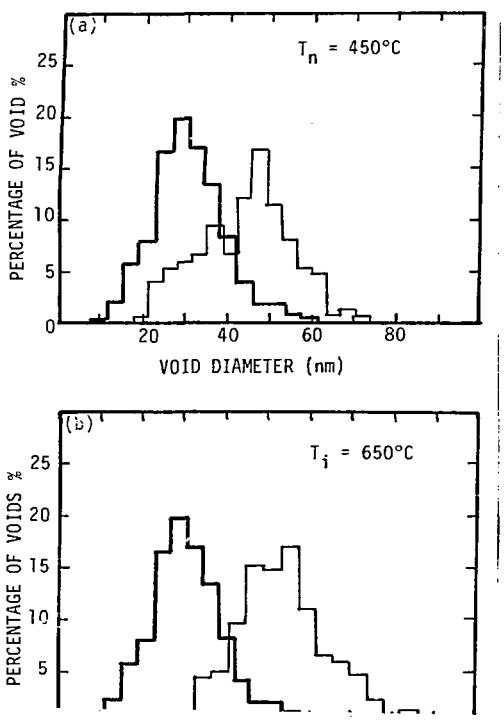

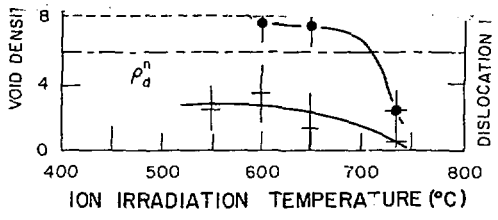

Fig. 5. Void number density and dislocation density for specimens preconditioned at 450°C and Ni ion irradiated to 60 dpa. Broken lines indicate the levels attained during neutron irradiation.

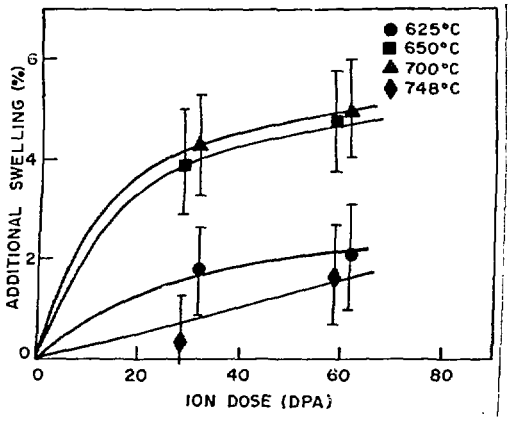

Fig. 7. Additional swelling produced during 4 MeV Ni ion irradiation of SA 316 after prior neutron irradiation at 585°C.

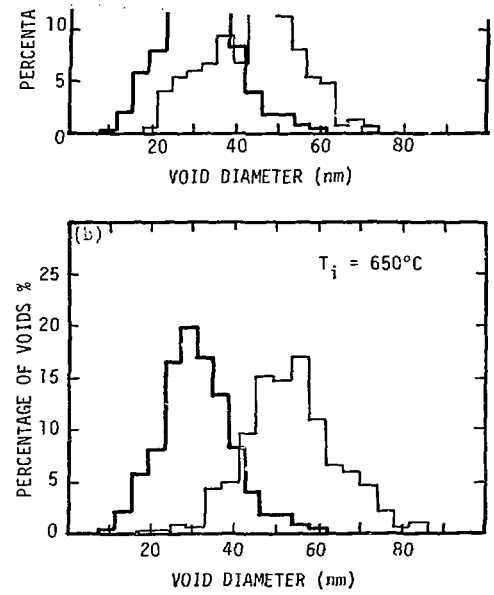

Fig.6. Changes in void size distribution with displacement dose. Initial distribution produced by neutron irradiation to 8×10^{22} n·cm^{-2} at 450°C is *illustrated in heavy lines*: (a) change produced by further neutron irradiation to 12×10^{22} n·cm^{-2} at 450°C and (b) change produced by further ion irradiation to 60 dpa at 650°C.

3

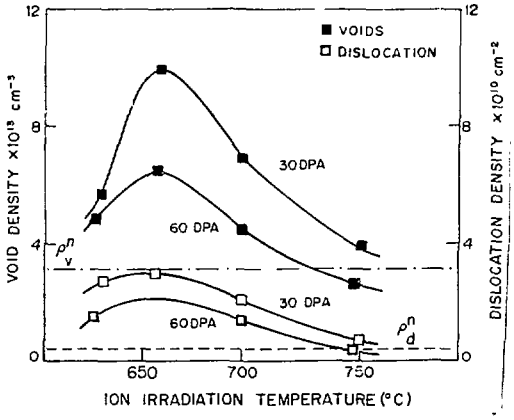

Fig. 8. Void number density and dislocation density for specimens preconditioned at 585°C and Ni ion irradiated to 30 and 60 dpa. Broken lines indicate the levels attained during neutron irradiation.

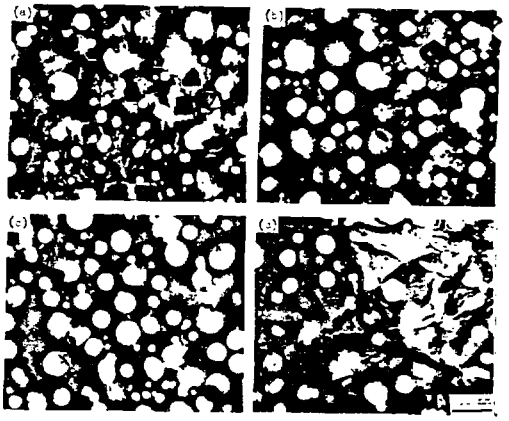

Fig. 9. Transmission electron micrographs illustrating precipitate dissolution: (a) neutron irradiated at 585°C and after subsequent Ni ion irradiation to 60 dpa at (b) 625°C, (c) 700°C, and (d) 750°C.

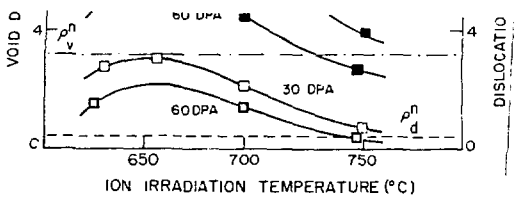

Fig. 8. Void number density and dislocation density for specimens preconditioned at 585°C and Ni ion irradiated to 30 and 60 dpa. Broken lines indicate the levels attained during neutron irradiation.

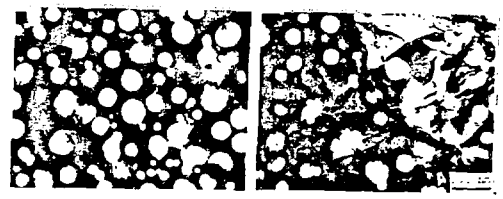

Fig. 9. Transmission electron micrographs illustrating precipitate dissolution: (a) neutron irradiated at 585°C and after subsequent Ni ion irradiation to 60 dpa at (b) 625°C, (c) 700°C, and (d) 750°C.

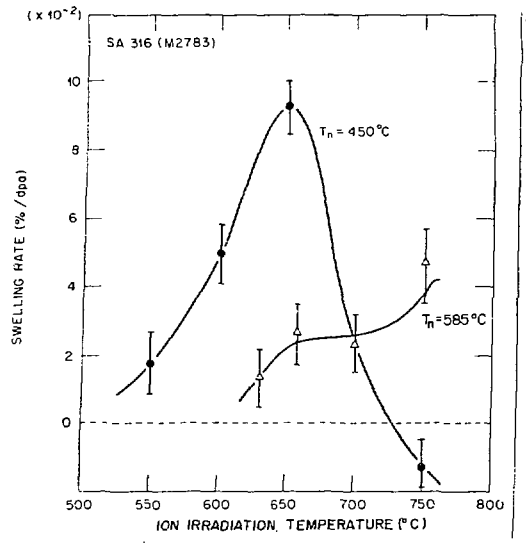

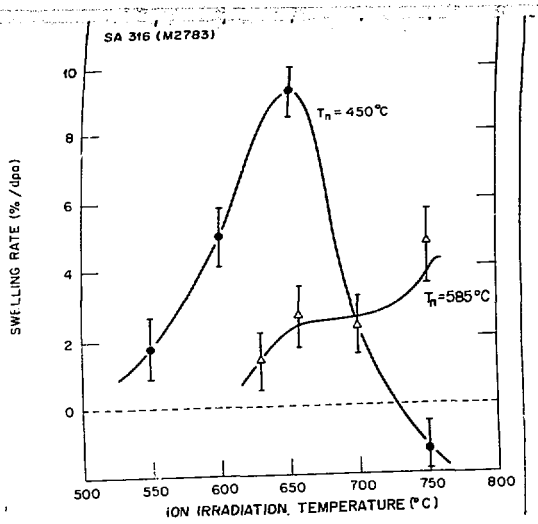

Fig. 10. Swelling rate versus ion irradiation temperature for specimens previously neutron irradiated at 450 and 585°C to a fluence of 8×10^{22} n·cm^{-2}.